Target Density Effects on Charge Transfer of Laser-Accelerated Carbon Ions in Dense Plasma

Jieru Ren,[1,*] Bubo Ma,[1,*] Lirong Liu,[1] Wenqing Wei,[1] Benzheng Chen,[1] Shizheng Zhang,[1] Hao Xu,[1] Zhongmin Hu,[1] Fangfang Li,[1] Xing Wang,[1] Shuai Yin,[1] Jianhua Feng,[1] Xianming Zhou,[1] Yifang Gao,[1] Yuan Li,[1] Xiaohua Shi,[1] Jianxing Li,[1] Xueguang Ren,[1] Zhongfeng Xu,[1] Zhigang Deng,[2] Wei Qi,[2] Shaoyi Wang,[2] Quanping Fan,[2] Bo Cui,[2] Weiwu Wang,[2] Zongqiang Yuan,[2] Jian Teng,[2] Yuchi Wu,[2] Zhurong Cao,[2] Zongqing Zhao,[2] Yuqiu Gu,[2] Leifeng Cao,[3] Shaoping Zhu,[2,4,5] Rui Cheng,[6] Yu Lei,[6] Zhao Wang,[6] Zexian Zhou,[6] Guoqing Xiao,[6,7] Hongwei Zhao,[6] Dieter H. H. Hoffmann,[1] Weimin Zhou,[2,†] and Yongtao Zhao[1,‡]

[1]*MOE Key Laboratory for Nonequilibrium Synthesis and Modulation of Condensed Matter, School of Physics, Xi'an Jiaotong University, Xi'an 710049, China*

[2]*Science and Technology on Plasma Physics Laboratory, Laser Fusion Research Center, China Academy of Engineering Physics, Mianyang 621900, China*

[3]*Advanced Materials Testing Technology Research Center, Shenzhen University of Technology, Shenzhen, 518118, China*

[4]*Institute of Applied Physics and Computational Mathematics, Beijing 100094, China*

[5]*Graduate School, China Academy of Engineering Physics, Beijing 100088, China*

[6]*Institute of Modern Physics, Chinese Academy of Sciences, Lanzhou 730000, China*

[7]*School of Nuclear Science and Technology, University of Chinese Academy Sciences, Beijing 101408, China*

(Received 1 August 2022; revised 16 December 2022; accepted 23 January 2023; published 27 February 2023)

We report on charge state measurements of laser-accelerated carbon ions in the energy range of several MeV penetrating a dense partially ionized plasma. The plasma was generated by irradiation of a foam target with laser-induced hohlraum radiation in the soft x-ray regime. We use the tricellulose acetate ($C_9H_{16}O_8$) foam of 2 mg/cm^3 density and 1 mm interaction length as target material. This kind of plasma is advantageous for high-precision measurements, due to good uniformity and long lifetime compared to the ion pulse length and the interaction duration. We diagnose the plasma parameters to be $T_e = 17$ eV and $n_e = 4 \times 10^{20}$ cm^{-3}. We observe the average charge states passing through the plasma to be higher than those predicted by the commonly used semiempirical formula. Through solving the rate equations, we attribute the enhancement to the target density effects, which will increase the ionization rates on one hand and reduce the electron capture rates on the other hand. The underlying physics is actually the balancing of the lifetime of excited states versus the collisional frequency. In previous measurement with partially ionized plasma from gas discharge and *z* pinch to laser direct irradiation, no target density effects were ever demonstrated. For the first time, we are able to experimentally prove that target density effects start to play a significant role in plasma near the critical density of Nd-glass laser radiation. The finding is important for heavy ion beam driven high-energy-density physics and fast ignitions. The method provides a new approach to precisely address the beam-plasma interaction issues with high-intensity short-pulse lasers in dense plasma regimes.

DOI: 10.1103/PhysRevLett.130.095101

Ion beam interaction with matter is a fundamental process involving complex atomic physics processes. It gets even more complex when the interacting ions and atoms are in a plasma environment. Accurately understanding the details of ion stopping in plasma is a prerequisite to make use of intense ion beams in high-energy-density physics [1–5]. It requires a correct knowledge of ion charge states when the ion traverses a dense plasma environment [6–10]. It is tempting to relate the charge state of an ion to the parameter Z_{eff} that appears in the stopping power theory,

$$-\frac{dE}{dx} \propto \frac{Z_{\mathrm{eff}}^2}{v^2} \times L, \tag{1}$$

where the energy loss (dE/dx) of heavy ions in the high-velocity range is determined by the square of the effective nuclear charge Z_{eff}, the Coulomb logarithm L, and the ion velocity v. Historically, Z_{eff}^2 is defined as the ratio of the heavy ion stopping $S_{(Z>1)}$ to the stopping of protons $S_{(Z=1)}$ at the same velocity v or at the same energy per nucleon (MeV/u) like $S_{(Z>1)}(v) = Z_{\mathrm{eff}}^2 S_{(Z=1)}(v)$. The energy loss of the projectile ion in a single collision is determined by the shielding of the nuclear charge [10,11]. The shielding depends on the impact parameter, the ion charge state, and the population of excited states. In a recent benchmark experiment, we were able to demonstrate the importance of excited ion states for the stopping process [12].

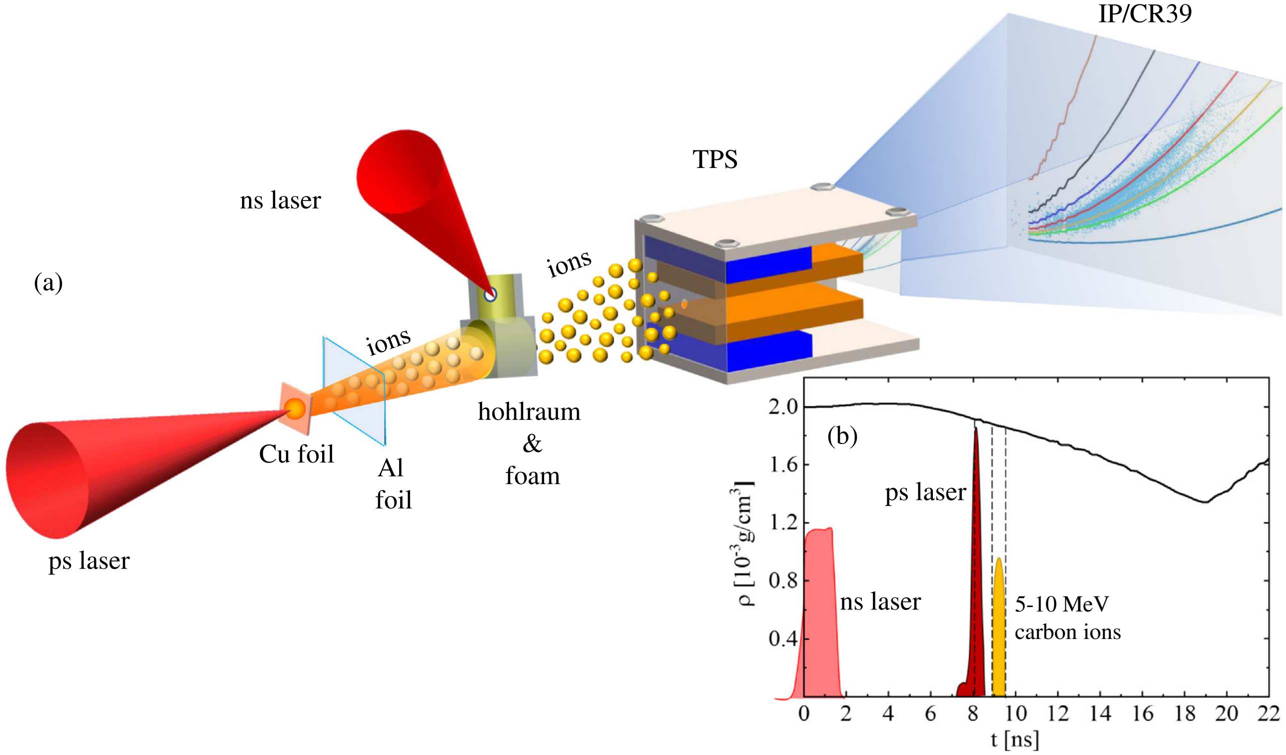

FIG. 1. Layout of the experiment. (a) A nanosecond laser is focused onto the inner wall of the Au hohlraum. The generated x rays from the hohlraum radiation heat the foam that is attached below the hohlraum into a plasma state. A picosecond laser is focused onto a copper foil, generating an intense short pulse of carbon ions through the TNSA mechanism. The Al foil between the copper foil and foam target protects the rear side of the copper foil against backscattering radiation from the nanosecond laser. After a flight distance of about 1.15 cm, the carbon ions interact with the plasma. The ions passing through the plasma are detected by a Thompson parabola spectrometer coupled to either an image plate (IP) or CR39. (b) The time sequence of the nanosecond laser pulse, picosecond laser pulse, and the ion-plasma interaction duration together with the plasma density evolution profile. The data for the density evolution are taken from Ref. [27].

When fast heavy ions pass through solid matter, the resulting charge state distribution is shifted to higher charge states compared to the situation when ions pass through the same line density of gaseous material [13–17]; the resulting energy loss is higher as well [18]. This finding is called density effects and can be well understood within the framework of the Bohr-Lindhard model [19], where the rapid succession of collisions populates excited states, which on the one hand increases the ionization probability due to the lower binding energy of excited states, and on the other hand decreases the shielding of the nuclear charge. Some experiments with gas discharge and pinch plasma have been performed since the 1990s. Higher charge states are observed when heavy ions penetrate plasma compared to the same amount of cold matter [20,21] because of the lower capture rate of free electrons. This in part also explains the observed enhanced stopping [12,22,23]. In these experiments, the plasma targets were limited in density up to some 10^{19} cm^{-3}, and the target density effects were never observed.

In recent years, the experiments shifted to higher density, where the plasma was created by direct heating of a target foil with an intense laser beam [24–26]. However, these plasma targets suffer from the drawback of steep gradients in density and temperature and they are highly transient phenomena. Moreover, traditional optical diagnostic methods are limited to the density corresponding to the critical density of the diagnostic laser. The determination of the properties of the warm dense matter, which is part of the heated target foil, relies strongly on simulations. These factors contribute to uncertainties in the analysis and the interpretation of the data. In our approach, we therefore used a long-living, well-characterized dense plasma. It was created by heating a CHO foam with laser generated hohlraum radiation in the soft x-ray regime [27–30]. This plasma sample has been successfully applied in previous experiments to explore the intense proton beam stopping process [31] and the laboratory observation of white dwarf-like matter [32].

Here we employed this plasma sample to measure the charge transfer process of laser-accelerated carbon ions in dense plasma. The plasma lifetime is approximately 10 ns, which is long compared to the duration of about 1 ps for the pulse length of the laser-accelerated carbon ions. This pulse length in the investigated energy region is longitudinally stretched to about 0.5 ns due to the momentum spread, when it interacts with the target. Therefore, the target conditions can be regarded as constant during the interaction time. This is a significant improvement compared to the situation with direct heated targets and therefore leads to higher precision data. The average charge states of the ions passing through the plasma were compared to theoretical predictions with semiempirical formula and by solving rate equations. These theories significantly misrepresent the experimental data when target density effects were not included. After modifying the rates of the relevant processes, namely, reducing the electron capture rates and increasing the Coulomb collision ionization rates, theoretical predictions agree well with our experimental data.

The experiment was performed at the XG-III laser facility of the Laser Fusion Research Center in Mianyang. The experimental layout is displayed in Fig. 1. The picosecond laser pulse of 130 J energy and 843 fs duration was focused onto a flat copper foil of 10 μm thickness to generate carbon ions through target normal sheath acceleration (TNSA) mechanism. Protons were accelerated simultaneously, but are not discussed here. To ensure the beam quality from TNSA, a secondary 10 μm Al foil was inserted to protect the rear side of the copper target from being heated by the nanosecond laser.

The target setup consists of a gold hohlraum converter (1 mm diameter, 1.9 mm length) with an attached tricellulose acetate ($C_9H_{16}O_8$) foam (2 mg/cm^3 density, 1 mm thickness). The nanosecond laser pulse of 150 J energy in 2 ns duration was incident upon the inner surface of the hohlraum to generate x rays, which subsequently heated the foam to plasma state. This kind of target scheme and the heating technique allows one to generate homogeneous, long-lasting dense plasma, which has been extensively studied at both PHELIX and XGIII laser facilities. The current target is the same as the one that was used in the previous experiments and details of the plasma diagnostic can be found there [27,28,31,32]. The temperature of the foam target was spectroscopically diagnosed to be 17 ± 1 eV with the Boltzmann plotting method. Supported by the FLYCHK program, the ionization degree of the plasma is about $C^{3.8+}H^{0.98+}O^{4.5+}$. Within reasonable assumption of constant mass density of 2 mg/cm^3, the free electron density of $(4.0 \pm 0.3) \times 10^{20}$ cm^{-3} was determined.

The picosecond laser was triggered at about 8 ns after the start of the nanosecond laser. The carbon ions were generated from the rear side of the copper target with TNSA mechanism in picosecond following the laser pulse. After a flight distance of about 1.15 cm, they reached the foam target. The carbon ions in the investigated range of 5–10 MeV interact with the plasma in the time span between 8.9 and 9.4 ns, when the foam was already fully heated, but no macroexpansion has occurred yet. The ion-plasma interaction time is on the order of 0.5 ns. This is 1 order of magnitude shorter than the timescale for the hydrodynamic response of the target. Therefore, the target can be regarded as stationary for our measurement.

The energies of the carbon ions traversing the plasma were measured with a Thomson parabola spectrometer

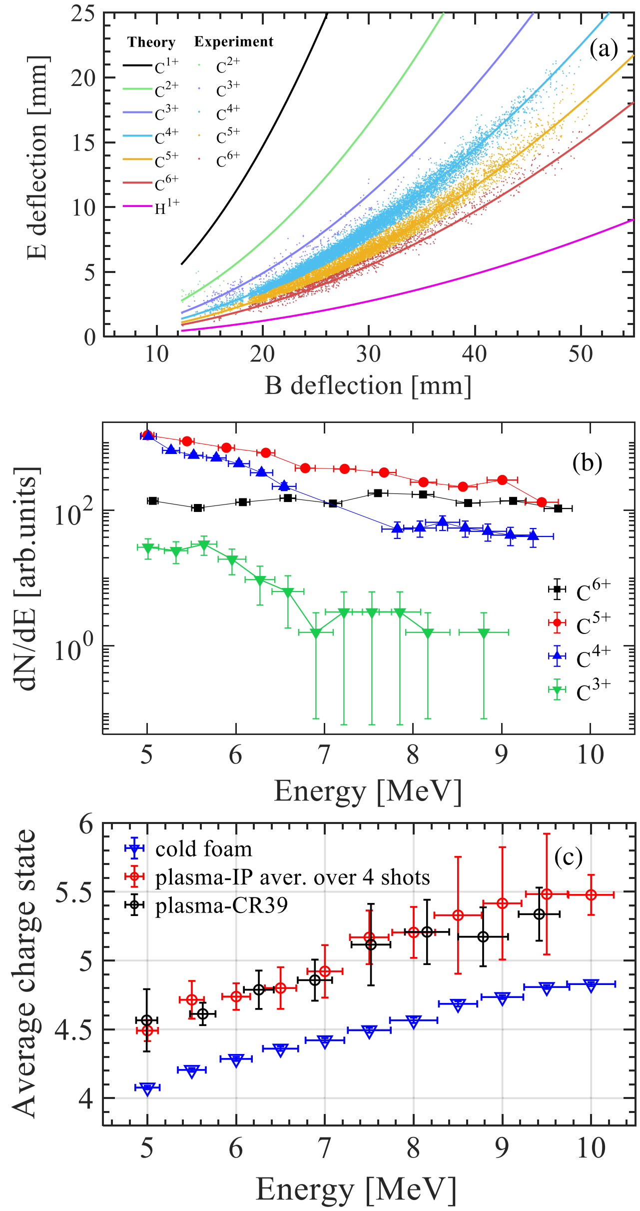

FIG. 2. TPS CR39 tracks of carbon ions passing through the plasma and the converted energies spectra as well as the calculated average charge states. (a) TPS CR39 tracks of carbon ions passing through the plasma and the theoretical deflection curves. (b) The converted energy spectra of carbon ions passing through the plasma. (c) The average charge state for carbon ions penetrating plasma and cold foam.

(TPS) coupled to either a Fuji image plate or a plastic track detector CR39. The typical tracks of the carbon ions obtained by CR39 are shown in Fig. 2(a) by dots, where the X and Y coordinates represent the magnetic and electric deflection distances relative to the zero order. The solid curves from upper left to bottom right are the theoretical deflection distance of ion species from C^{1+} to C^{6+} and H^{1+}. The experimental tracks for protons and the zero order resulting from neutral particles are excluded in this figure.

The small gap at the B deflection distance of about 18 mm is due to the unetched border of the CR39.

The experimental tracks of carbon ions displayed in Fig. 2(a) were converted to energies according to the deflection distance. The energy spectra are shown in Fig. 2(b). The error bars of the intensity in the Y direction represent the statistical errors, and the error bars of energy in the X direction represent actually the energy resolution of the TPS. According to the energy spectra in Fig. 2(b), the energy-dependent average charge states $\bar{Z}(E) = \sum_q P_q(E) Z_q$ are calculated and shown in Fig. 2(c), where $P_q(E)$ is the probability of carbon ion in charge state Z_q, and E is the kinetic energy of carbon ion. The error bars of energy in the X direction represent the energy resolution of the TPS for the ion species that has the lowest resolution. The error bars of the average charge state in the Y direction for the plasma case measured with the CR39 detector originate from the statistical errors and ion distinguishment error. To present the representativeness and repeatability of the result, the average charge states of the plasma case averaged over another 4 shots measured with the image plate are shown as well, with error bars representing the statistical error and shot-to-shot fluctuations. The data measured in different shots with either the image plate or CR39 agree with each other very well. Additionally, the average charge states of carbon ions passing through cold foam are also presented. More experimental details can be found in Supplemental Material [33]. Higher charge states are observed for carbon ions penetrating plasmas compared to that in the cold foam because of “plasma effects” that have been observed in a lot of experiments [20,21]. In this Letter, we focused on the “target density effect” that enhanced the charge states even above the plasma effect expectation.

According to the model of Morales *et al.* [34], the equilibrium length of the investigated carbon ions in the experimentally used plasma is about 0.1 mm. This is 1 order of magnitude lower than the plasma scale. Hence, the measured charge states can be reasonably regarded as the equilibrium charge states of the outgoing carbon ions. In Fig. 3, the average charge states of carbon ions traversing the plasma were compared to theoretical predictions by the analytical formula proposed by Kreussler *et al.* [35] and Gus’kov *et al.* [36]. These two models are based on Bohr’s stripping criterion [37] while replacing the ion velocity by the average relative ion velocity with respect to the target electrons. The model of Gus’kov *et al.*, which describes the plasma electron motion with the Fermi-Dirac function, underestimates our experimental data by about 30%. The model of Kreussler *et al.*, which takes into account the thermal velocity distribution of the plasma electrons, predicts higher charge states than the model of Gus’kov *et al.*, but still underestimates the experimental data.

In order to understand this discrepancy, we solved the rate equations by taking into consideration the dominant charge transfer processes such as Coulomb ionization by plasma ions and free electrons, capture of bound electrons, capture of free electrons, and three-body recombination processes [33]. The photoionization, dielectronic recombination, and multielectron processes are neglected. The rates for the above charge transfer processes are calculated according to the models reported by Peter and Meyer-ter-Vehn [7] and the references therein [38–45]. As shown in Fig. 3, the calculated equilibrium average charge states without (blue dotted curve) target density effects greatly underestimate the experimental results. Good agreements are achieved between the rate equation predictions (blue solid curve) and experimental data when the target density effects are taken into account.

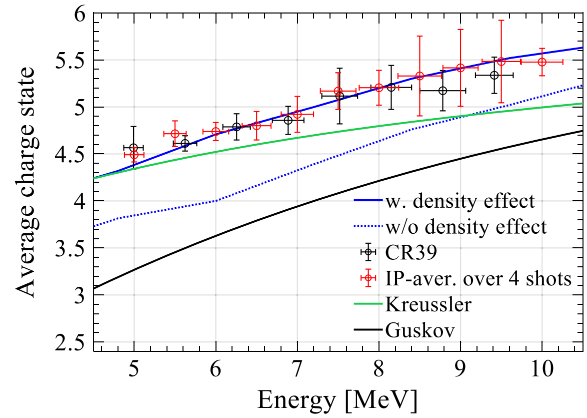

FIG. 3. Comparison of the measured average charge state of carbon ions passing through the plasma and the theoretical predictions by analytical formula, solving rate equations with and without target density effects.

The typical rates of the charge transfer processes for 6 MeV carbon ions in the experimentally used plasma are shown in Fig. 4(a). The dashed curves represent the results in the framework of two-body collisions, where the rate coefficients are density independent. The solid curves represent the results with target density effect modifications. The equilibrium charge state Z_{eq} is achieved when the electron loss rate equals the electron recombination rate, hence the intersection of the electron ionization and capture curves denotes the value of Z_{eq}. The values of the Z_{eq} with and without target density effects are marked in Fig. 4(a). When the target density effects are considered, the average equilibrium charge state is enhanced by about 18% from 4.0 to 4.7. As shown in Fig. 3, in the investigated energy range from 5 to 10 MeV, when the target density effects are considered, the average charge states are considerably enhanced and agree with our experimental data very well. The target density effects are discussed in more detail below.

In dense plasmas, the captured electrons, especially those in highly excited states, might experience secondary collisions before deexcitation takes place and they therefore can be easily ionized. In this way, the electron capture possibilities are reduced and the ion charge states are enhanced. As shown in Fig. 4(a), when the target density effect is taken into account, considerable reduction occurs for the electron

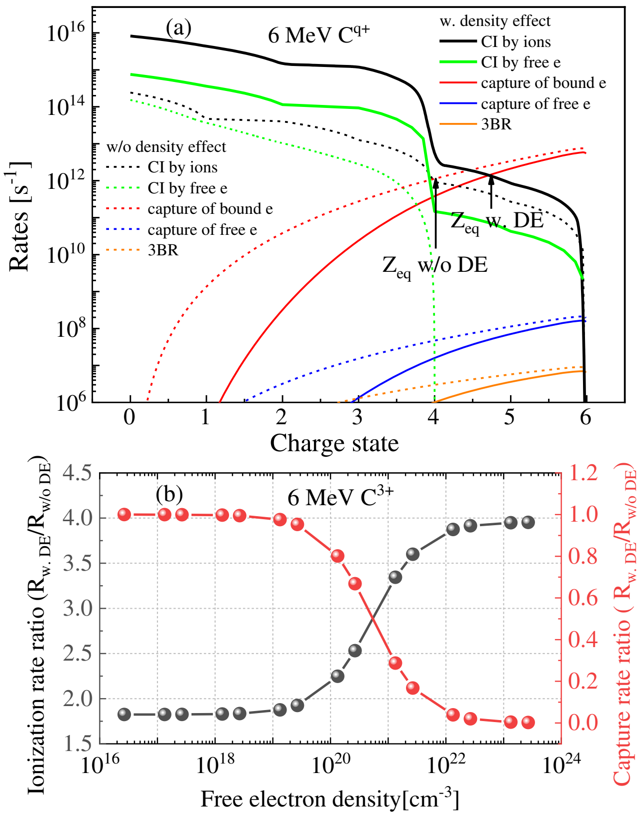

FIG. 4. Rate coefficients for charge transfer processes of 6 MeV carbon ions interacting with the experimentally used plasma. (a) Typical rate coefficients for the Coulomb ionization (CI) by plasma ions (black curves), Coulomb ionization by free electrons (green curves), capture of bound electrons (red curves), capture of free electrons or radiative electron capture in another word (blue curves), and three-body recombination (3BR) processes (orange curves) with (solid curves) and without (dashed curves) target density effects (DEs). (b) Ratio of the charge transfer rates with and without target density effects modifications versus the target density.

capture processes, including bound electron capture, free electron capture, and three-body recombination.

In addition, the frequent succession of collisions in dense plasma gives rise to the two-step processes, excitation, and subsequent ionization. This process increases the electron ionization possibilities and leads to the enhancement of the ion charge state. As shown in Fig. 4(a), when the target density effect is considered, the Coulomb ionization rates, either by plasma ions or by free electrons, are drastically enhanced.

Therefore, we conclude that, in the current case of $n_e = 4 \times 10^{20}$ cm^{-3}, the target density effects significantly decrease the electron capture rates and increase the electron loss rates. Consequently, the equilibrium average charge states are enhanced. The ratios of the electron capture/loss rates with and without target density effects as a function of free electron density are shown in Fig. 4(b). In the calculations, the plasma was assumed to be partially ionized with the same ionization rates as the experimentally used sample. The results imply that the target density effects start to play an important role at electron density of about 10^{19} cm^{-3}. The underlying fundamental physics is actually the balancing of the lifetime of excited states versus the collisional frequency. Only when the lifetime of the excited state is larger than the collisional timescale will the target density effects play important roles. Our experiments exactly step into this regime and provide the experimental evidence.

In summary, the charge states of laser-accelerated carbon ions passing through the dense plasma were measured. By taking advantage of the uniform quasistatic plasma target and short-pulse projectile, high-precision experimental data were obtained. This allows one to distinguish between various models. The experimental data exceed the predictions of the Gus'kov and Kreussler analytical models, as well as the rate equation solutions in case that target density effects are not included. With the increase of target density, the lifetime of the excited states approaches and even exceeds the collisional timescale. In these cases, the target density effect will, on one hand, reduce the electron capture rate and, on the other hand, increase the Coulomb ionization rate. As a result, considerable increase of the charge state is expected. Theoretical predictions of rate equations considering the target density effects well reproduce our experimental results. This is the first experimental evidence pinning down that target density effects start to play a significant role in near critical density plasma and is an example of a precise benchmark measurement of complex processes. The results are significant for an accurate understanding of ion-plasma interaction, which is essential for the physical design of heavy ion beam driven high-energy-density physics and fast ignitions. In the future, the method can also be applied in high-energy-density physics and laboratory astrophysics in a broader range.

We sincerely thank the staff from Laser Fusion Research Center, Mianyang for the laser system running and target fabrication. The work was supported by National Key R&D Program of China (No. 2019YFA0404900 and No. 2022YFA1603300), National Natural Science Foundation of China (Grants No. 12120101005, No. U2030104, No. 12175174, and No. 11975174), Chinese Science Challenge Project No. TZ2016005, China Postdoctoral Science Foundation (No. 2017M623145), State Key Laboratory Foundation of Laser Interaction with Matter (No. SKLLIM1807 and No. SKLLIM2106), the Fundamental Research Funds for the Central Universities, and Young Talent Fund of Association for Science and Technology in Shaanxi, China.

[*]J. R. and B. M. have contributed equally to this work.
[†]Corresponding author.
zhouwm@caep.cn

‡Corresponding author.
zhaoyongtao@xjtu.edu.cn

[1] A. Pelka *et al.*, Ultrafast Melting of Carbon Induced by Intense Proton Beams, Phys. Rev. Lett. **105**, 265701 (2010).

[2] P. K. Patel, Andrew Mackinnon, M. H. Key, T. E. Cowan, M. E. Foord, M. Allen, D. Price, H. Ruhl, P. T. Springer, and R. B. Stephens, Isochoric Heating of Solid-Density Matter with an Ultrafast Proton Beam, Phys. Rev. Lett. **91**, 125004 (2003).

[3] K. Schoenberg *et al.*, High-energy-density-science capabilities at the facility for antiproton and ion research, Phys. Plasmas **27**, 043103 (2020).

[4] J. Ren, C. Maurer, P. Katrik, P. M. Lang, A. A. Golubev, V. Mintsev, Y. Zhao, and D. H. H. Hoffmann, Accelerator-driven high-energy-density physics: Status and chances, Contrib. Plasma Phys. **58**, 82 (2018).

[5] Claude Deutsch and Gilles Maynard, Ion stopping in dense plasmas: a basic physics approach, Matter Radiat. Extrem. **1**, 6 (2016).

[6] A. Frank, A. Blažević, V. Bagnoud, M. M. Basko, M. Börner, W. Cayzac, D. Kraus, T. Heßling, D. H. H. Hoffmann, A. Ortner, A. Otten, A. Pelka, D. Pepler, D. Schumacher, An. Tauschwitz, and M. Roth, Energy Loss and Charge Transfer of Argon in a Laser-Generated Carbon Plasma, Phys. Rev. Lett. **110**, 115001 (2013).

[7] Thomas Peter and Jürgen Meyer-ter-Vehn, Energy loss of heavy ions in dense plasma. II. Nonequilibrium charge states and stopping powers, Phys. Rev. A **43**, 2015 (1991).

[8] Manuel D. Barriga-Carrasco, David Casas, and Roberto Morales, Calculations on charge state and energy loss of argon ions in partially and fully ionized carbon plasmas, Phys. Rev. E **93**, 033204 (2016).

[9] A. Ortner, A. Frank, A. Blažević, and M. Roth, Role of charge transfer in heavy-ion-beam–plasma interactions at intermediate energies, Phys. Rev. E **91**, 023104 (2015).

[10] O. N. Rosmej, A. Blazevic, S. Korostiy, R. Bock, D. H. H. Hoffmann, S. A, Pikuz, V. P. Efremov, V. E. Fortov, A. Fertman, T. Mutin, T. A. Pikuz, and A. Ya. Faenov, Charge state and stopping dynamics of fast heavy ions in dense matter, Phys. Rev. A **72**, 052901 (2005).

[11] J. I. Juaristi, A. Arnau, P. M. Echenique, C. Auth, and H. Winter, Charge State Dependence of the Energy Loss of Slow Ions in Metals, Phys. Rev. Lett. **82**, 1048 (1999).

[12] Y. T. Zhao, Y. N. Zhang, R. Cheng, B. He, C. L. Liu, X. M. Zhou, Y. Lei, Y. Y, Wang, J. R. Ren, X. Wang, Y. H. Chen, G. Q. Xiao, S. M. Savin, R. Gavrilin, A. A. Golubev, and D. H. H. Hoffmann, Benchmark Experiment to Prove the Role of Projectile Excited States upon the Ion Stopping in Plasmas, Phys. Rev. Lett. **126**, 115001 (2021).

[13] N. O. Lassen, The total charges of fission fragments in gaseous and solid stopping media, Dan. Mat. Fys. Medd. **26**, 1 (1951).

[14] H. Ogawa *et al.*, Gas-solid difference in charge-changing cross sections for bare and H-like nickel ions at 200 MeV/u, Phys. Rev. A **75**, 020703(R) (2007).

[15] S. Eisenbarth, O. N. Rosmej, V. P. Shevelko, A. Blazevic, and D. H. H. Hoffmann, Numerical simulations of the projectile ion charge difference in solid and gaseous stopping matter, Laser Part. Beams **25**, 601 (2007).

[16] V. P. Shevelko, O. Rosmej, H. Tawara, and I. Y. Tolstikhina, The target-density effect in electron-capture processes, J. Phys. B **37**, 601 (2007).

[17] V. P. Shevelko, O. Rosmej, H. Tawara, and I. Yu Tolstikhina, The target-density effect in electron-capture processes, J. Phys. B **37**, 201 (2003).

[18] H. Geissel, Y. Laichter, W. F. W. Schneider, and P. Armbruster, Energy loss and energy loss straggling of fast heavy ions in matter, Nucl. Instrum. Methods Phys. Res. **194**, 21 (1982).

[19] N. O. Lassen, Electron capture and loss by heavy ions penetrating through matter, Dan. Mat. Fys. Medd. **28**, 1 (1954).

[20] K.-G. Dietrich, D. H. H. Hoffmann, E. Boggasch, J. Jacoby, H. Wahl, M. Elfers, C. R. Haas, V. P. Dubenkov, and A. A. Golubev, Charge State of Fast Heavy Ions in a Hydrogen Plasma, Phys. Rev. Lett. **69**, 3623 (1992).

[21] Ge Xu *et al.*, Determination of Hydrogen Density by Swift Heavy Ions, Phys. Rev. Lett. **119**, 204801 (2017).

[22] J. Jacoby, D. H. H. Hoffmann, W. Laux, R. W. Müller, H. Wahl, K. Weyrich, E. Boggasch, B. Heimrich, C. Stöckl, H. Wetzler, and S. Miyamoto, Stopping of Heavy Ions in a Hydrogen Plasma, Phys. Rev. Lett. **74**, 1550 (1995).

[23] D. H. H. Hoffmann, K. Weyrich, H. Wahl, D. Gardés, R. Bimbot, and C. Fleurier, Energy loss of heavy ions in a plasma target, Phys. Rev. A **42**, 2313 (1990).

[24] W. Cayzac, A. Frank, A. Ortner, V. Bagnoud, M. M. Basko, S. Bedacht, C. Bläser, A. Blažvić, S. Busold, O. Deppert *et al.*, Experimental discrimination of ion stopping models near the Bragg peak in highly ionized matter, Nat. Commun. **8**, 15693 (2017).

[25] M. Gauthier *et al.*, Charge Equilibrium of a Laser-Generated Carbon-Ion Beam in Warm Dense Matter, Phys. Rev. Lett. **110**, 135003 (2013).

[26] J. Braenzel, M. D. Barriga-Carrasco, R. Morales, and M. Schnürer, Charge-Transfer Processes in Warm Dense Matter: Selective Spectral Filtering for Laser-Accelerated Ion Beams, Phys. Rev. Lett. **120**, 184801 (2018).

[27] O. N. Rosmej, N. Suslov, D. Martsovenko, G. Vergunova, N. Borisenko, N. Orlov, T. Rienecker, D. Klir, K. Rezack, A. Orekhov *et al.*, The hydrodynamic and radiative properties of low-density foams heated by x-rays, Plasma Phys. Controlled Fusion **57**, 094001 (2015).

[28] Bubo Ma *et al.*, Plasma spectroscopy on hydrogen-carbon-oxygen foam targets driven by laser-generated hohlraum radiation, Laser Part. Beams **2022**, 3049749 (2022).

[29] Steffen Faik, Anna Tauschwitz, Mikhail M. Basko, Joachim A. Maruhn, Olga Rosmej, Tim Rienecker, Vladimir G. Novikov, and Alexander S. Grushin, Creation of a homogeneous plasma column by means of hohlraum radiation for ion-stopping measurements, High Energy Density Phys. **10**, 47 (2014).

[30] O. N. Rosmej, V. Bagnoud, U. Eisenbarth, V. Vatulin, N. Zhidkov, N. Suslov, A. Kunin, A. Pinegin, D. Schäfer, Th. Nisius *et al.*, Heating of low-density CHO-foam layers by means of soft x-rays, Nucl. Instrum. Methods Phys. Res., Sect. A **653**, 52 (2011).

[31] Jieru Ren *et al.*, Observation of a high degree of stopping for laser-accelerated intense proton beams in dense ionized matter, Nat. Commun. **11**, 5157 (2020).

[32] Bu-Bo Ma *et al.*, Laboratory observation of C and O emission lines of the white dwarf $H1504 + 65$-like atmosphere model, Astrophys. J. **920**, 106 (2021).

[33] See Supplemental Material at http://link.aps.org/supplemental/10.1103/PhysRevLett.130.095101 for more experimental details as well as the theoretical calculations of the charge transfer processes and the target density effects.

[34] Roberto Morales, Manuel D. Barriga-Carrasco, and David Casas, Instantaneous charge state of uranium projectiles in fully ionized plasmas from energy loss experiments, Phys. Plasmas **24**, 042703 (2017).

[35] S. Kreussler, C. Varelas, and Werner Brandt, Target dependence of effective projectile charge in stopping powers, Phys. Rev. B **23**, 82 (1981).

[36] S. Yu. Gus'kov, N. V. Zmitrenko, D. V. Il'in, A. A. Levkovskii, V. B. Rozanov, and V. E. Sherman, A method for calculating the effective charge of ions decelerated in a hot dense plasma, Plasma Phys. Rep. **35**, 709 (2009).

[37] N. Bohr, Velocity-range relation for fission fragments, Phys. Rev. **59**, 270 (1941).

[38] Michal Gryziński, Classical theory of atomic collisions. I. Theory of inelastic collisions, Phys. Rev. **138**, A336 (1965).

[39] Michał Gryziński, Two-particle collisions. I. General relations for collisions in the laboratory system, Phys. Rev. **138**, A305 (1965).

[40] Wolfgang Lotz, An empirical formula for the electron-impact ionization cross-section, Z. Phys. **206**, 205 (1967).

[41] J Robert Oppenheimer, On the quantum theory of the capture of electrons, Phys. Rev. **31**, 349 (1928).

[42] H. C. Brinkmann and H. A. Kramers, Theory of the emission of electrons by alpha-particles, Proc. K. Ned. Akad. Wet **33**, 973 (1930).

[43] Hans D Betz, Heavy ion charge states, Appl. At. Collision Phys. **4**, 2 (1983).

[44] Th. Peter, Scaling laws for the effective charge of heavy ions penetrating gas or plasma targets, Laser Part. Beams **8**, 643 (1990).

[45] Ya. B. Zel'Dovich and Yu. P. Raizer, *Physics of Shock Waves and High-Temperature Hydrodynamic Phenomena* (Academic Press, New York, 1966), Vol. 1.